Light Metals 2013 *Edited by: Barry Sadler*
TMS (The Minerals, Metals & Materials Society), 2013

EFFECT OF IRON IN Al-Mg-Si-Mn DUCTILE DIECAST ALLOY

S. Ji[1], W. Yang[1], F. Gao[1], D. Watson[1,2], Z. Fan[1]

[1]Brunel Centre for Advanced Solidification Technology (BCAST), Brunel University, Uxbridge, Middlesex, UB8 3PH, United Kingdom
[2]Engineering Centre, Jaguar Cars Ltd, Abbey Road, Coventry, CV34 4LF, United Kingdom

Keywords: Aluminium alloy, mechanical properties, Fe-rich compounds, high pressure die casting, CALPHAD

Abstract

The effect of iron on the microstructure and mechanical properties of Al-Mg-Si-Mn alloys has been investigated in high pressure diecast components in association with CALPHAD modelling of the multi-component Al-Mg-Si-Mn-Fe system. It is found that the Fe-rich intermetallic phases solidify in two stages in the high pressure die casting process: one is in the shot sleeve and the other is in the die cavity, showing different morphologies. The compact and star-like intermetallics are identified as α-AlFeMnSi phase with typical composition of $Al_{12}(Fe,Mn)_3Si$. At the increased level of Fe content, β-AlFe is found in the microstructure with a long needle-shaped morphology, which is identified as $Al_{13}(Fe,Mn)_4Si_{0.25}$. The existence of Fe-rich intermetallics in the alloy slightly increases the yield strength, but significantly reduces the elongation. The ultimate tensile strength maintains at similar levels when Fe contents are less than 0.6wt.%, but decreases significantly with the further increased Fe concentration in the alloys.

Introduction

In diecast alloys, iron is a common impurity element as it is unavoidably picked up in practice. This is mainly resulted from the use of steel tools during melting and casting, and particularly when the scraped and recycled materials are used. In high pressure die casting (HPDC) process, the presence of iron is beneficial to prevent die soldering [1,2], but the excessive Fe has been found to be detrimental to the mechanical properties of Al-Si, Al-Si-Cu and Al-Si-Mg alloys [3,4]. The detrimental effect is due to its low equilibrium solubility in the α-Al solid phase (<0.04wt.%[3]) and the associated strong tendency to form various low symmetry Al-Fe or Al-Fe-Si intermetallic phases. The effect of Fe-rich intermetallic phases in aluminium alloys on the mechanical properties depends on their type, size and amount in the microstructure. In order to diminish the detrimental effect of iron, several metallurgical solutions are effectively used, which include (1) to avoid the formation of low symmetry Al-Fe or Al-Fe-Si compounds by lowering the Fe levels as low as economically possible; (2) to modify the crystal structures from low symmetry compounds to high symmetry lattice types in castings; (3) to refine the intermetallics by physical approaches including the use of superheated melt, solidification under high cooling rate, and/or melt treatment [5], or by chemical approaches to add Ca or Sr elements prior to solidification [6]; and (4) to spheroidise the needle or plate-shaped Fe-rich intermetallics using non-equilibrium heat treatment of castings [7].

In Al-Si-Fe system there are five main Fe-rich phases: Al_3Fe (or $Al_{13}Fe_4$), α-Al_8Fe_2Si (possibly α-$Al_{12}Fe_3Si_2$), β-Al_5FeSi, δ-Al_4FeSi_2 and γ-Al_3FeSi [8,9]. For the cast hypoeutectic Al-Si alloys containing Fe, Mn and Mg [12], three Fe-rich phases of α-$Al_{15}(FeMn)_3Si_2$, β-Al_5FeSi and π-$Al_8FeMg_3Si_6$ compounds have been identified in normal compositions. Among the intermetallics, β-Al_5FeSi usually appears as highly faceted platelets up to several millimetres and it therefore causes the most serious loss of strength and ductility in the castings [10, 11]. In particular, the α-Al_8Fe_2Si phase has been reported as the compounds with many different types of morphology [12, 13]. The morphological changes from plate to Chinese script or compact shapes were reported to enhance mechanical properties [14, 15].

The formation of Fe-rich intermetallics is greatly affected by solidification conditions during casting. The superheat and cooling rate have been reported to affect the nucleation and growth of the Fe-rich phases and thus to be able to modify the morphology and size of the intermetallics in aluminium alloys [21]. It was also reported that the refinement and fragmentation of β-AlFeSi platelets can be achieved by rapid solidification [16,17]. The precipitation of β-AlFeSi phase can be hindered by high cooling rate, which retains Fe in solid solution and suppresses the formation of the primary β-AlFeSi phase [18,19].

The present study attempts to investigate the effect of Fe on the morphology, size and distribution of various Fe-rich compounds in the ductile Al-Mg-Si-Mn alloy produced by HPDC process. The mechanical properties of yield strength, ultimate tensile strength and elongation were assessed with different Fe contents. The role of alloy chemistry on the effect of Fe was investigated by CALPHAD modelling of multi-component Al-Mg-Si-Mn-Fe system. The discussions are focused on the phase formation of different Fe-rich intermetallic phases and the relationship between Fe-rich compounds and mechanical properties of the diecast Al-Mg-Si-Mn alloy.

Experimental

The Al-Mg-Si-Mn alloys with different Fe contents were produced by melting the ingots of commercial pure aluminium, pure magnesium and the master alloys of Al-15wt.%Si, Al-20wt.%Mn, Al-10wt.%Ti and Al-80wt.%Fe. During the experiments, each element was weighed to a specified ratio with different extra amounts for burning loss compensation during melting. The 6-10kg melt was prepared in a clay-graphite crucible using an electric resistance furnace. The processing temperature of the melt ranged between 690 and 750°C. For all the experiments, the melt was subjected to fluxing and degassing using commercial fluxes and N_2. The N_2 degassing usually lasted

3 minutes and the granular flux covered on the top surface of the melt during N_2 degassing. The sample for composition analysis was taken from the melt after homogenisation.

Table 1 Compositions of diecast Al-Mg-Si-Mn alloys

Elements	Wt.%
Si	2.2±0.08
Fe	varied*
Mn	0.541±0.05
Mg	6.2±0.08
Ti	6.2±0.08
Zn	0.012±0.004
Others	<0.03
Al	bal.

* Actual Fe contents were measured to be 0.214, 0.389, 0.623, 0.841, 1.243, 1.490, 1.861, and 2.482, respectively.

A ϕ40×60mm cylindrical sample was made by casting the melt directly into a steel mould for the composition analysis. The casting was cut across the diameter at 15mm from the bottom and ground down to 800 grid abrasive grinding paper. The composition of each alloy was obtained from an optical mass spectroscopy, in which at least five spark analyses were performed and the average value was taken as the chemical composition of alloy. The composition was further confirmed by area energy dispersive X-ray (EDX) quantification in SEM. The actual compositions of the alloys are shown in Table 1.

After composition analysis and skimming, the melt was manually dosed and subsequently released into the shot sleeve of a 4500kN HPDC machine for the final casting, in which all casting parameters were fully monitored. The pouring temperature was measured by a K-type thermocouple, usually at 50°C above the liquidus of the alloy according to the equilibrium phase diagram. Six ASTM standard samples with three ϕ6.35mm round bar and three square bar were cast in each shot. The casting die was heated by the circulation of oil at 250°C. All castings were kept at ambient condition for at least 24 hours before the mechanical property test.

The tensile tests were conducted following the ASTM B557 standard using an Instron 5500 Universal Electromechanical Testing Systems equipped with Bluehill software and a ±50kN load cell. All the tests were performed at ambient temperature (~ 25°C). The gauge length of the extensometer was 25mm and the ramp rate for extension was 2mm/min. Each data reported is based on the properties obtained from 10 to 30 samples without showing obvious casting defects on the fractured surfaces.

The microstructure was examined using a Zeiss optical microscopy with quantitative metallography, and a Zeiss SUPRA 35VP scanning electron microscope (SEM), equipped with EDX. The particle size, volume fraction and the shape factor of the solid phase were measured using an AxioVision 4.3 Quantimet digital image analysis system. The quantitative EDX analysis in SEM was performed at an accelerating voltage of 20kV on a polished sample, and the libraries of standard X-ray profiles for EDX were generated using pure elements. In situ spectroscopy calibration was performed in each session of the EDX quantification using pure copper. To minimise the influence from the interaction volume during the EDX quantification, five point analyses on selected particles were conducted for each phase and the average was taken as the measurement.

Results

As-cast microstructure of the diecast Al-Mg-Si-Mn alloy

In the as-cast state, there was no significant change in the morphologies of the primary α-Al phase and eutectic phase presented in the Al-Mg-Si-Mn alloys containing different levels of Fe. However, the primary α-Al solid solution was found in two types of morphology in each alloy, which are labelled as 'α_1' and 'α_2' in Fig. 1, respectively. The α_1-Al phase was resulted from the solidification in the shot sleeve and exhibited dendrites and fragmented dendrites in the microstructure. The α_2-Al phase was formed during the solidification in the die cavity, which showed fine globular morphology. The sizes of dendritic and fragmented dendritic α_1-Al phase ranged from 20 to 100μm and the fine globular -Al particles ranged from 3 to 20μm. The coarse α_1-Al phase was isolated by fine globular α_2-Al particles. The interdendritic regions were characterised with a eutectic microstructure, in which the lamellar structure was made of α-Al and Mg_2Si phases. The primary α-Al phase was associated with the eutectic microstructure. Fe-rich intermetallic compounds were observed in the eutectic areas.

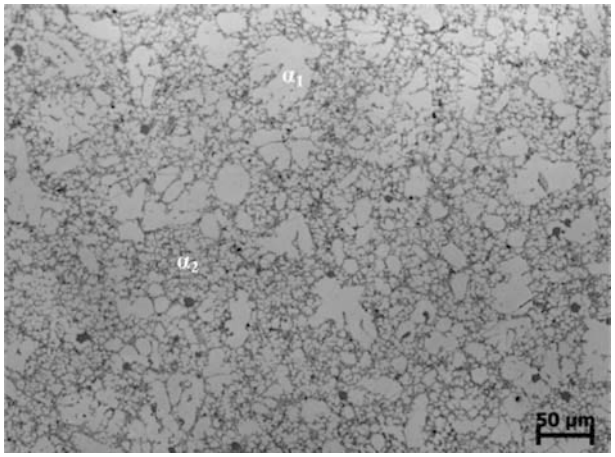

Figure 1. Microstructure of diecast Al-5wt.%Mg-2wt.%Si-0.54wt.%Mn diecast alloy with 0.62wt.%Fe.

In contrast to the primary α-Al phase, it is seen that the effect of Fe on the morphologies of primary Fe-rich compounds was significant. Different types and amounts of the Fe-rich intermetallics were related to the Fe and Mn contents, as shown in Fig. 2. From the experimental observations, only a small amount of fine intermetallic compounds were present in the alloys that contain up to 0.21wt.%Fe (Fig. 2a). The fine Fe-rich intermetallics were formed in the solidification inside the die cavity. Most of the fine intermetallics were located between the primary α-Al phases, although some intermetallics were found inside them. No primary Fe-rich intermetallic compounds were observed in the primary α-Al phase solidified in the shot sleeve. The EDX quantitive analysis by SEM identified the Fe-rich phase with the typical composition of the α-$Al_{12}(Fe,Mn)_3Si$ phase in the Al-Mg-Si-Mn-Fe system. No β-AlFe and β-AlFeSi intermetallics were observed in the samples at this composition.

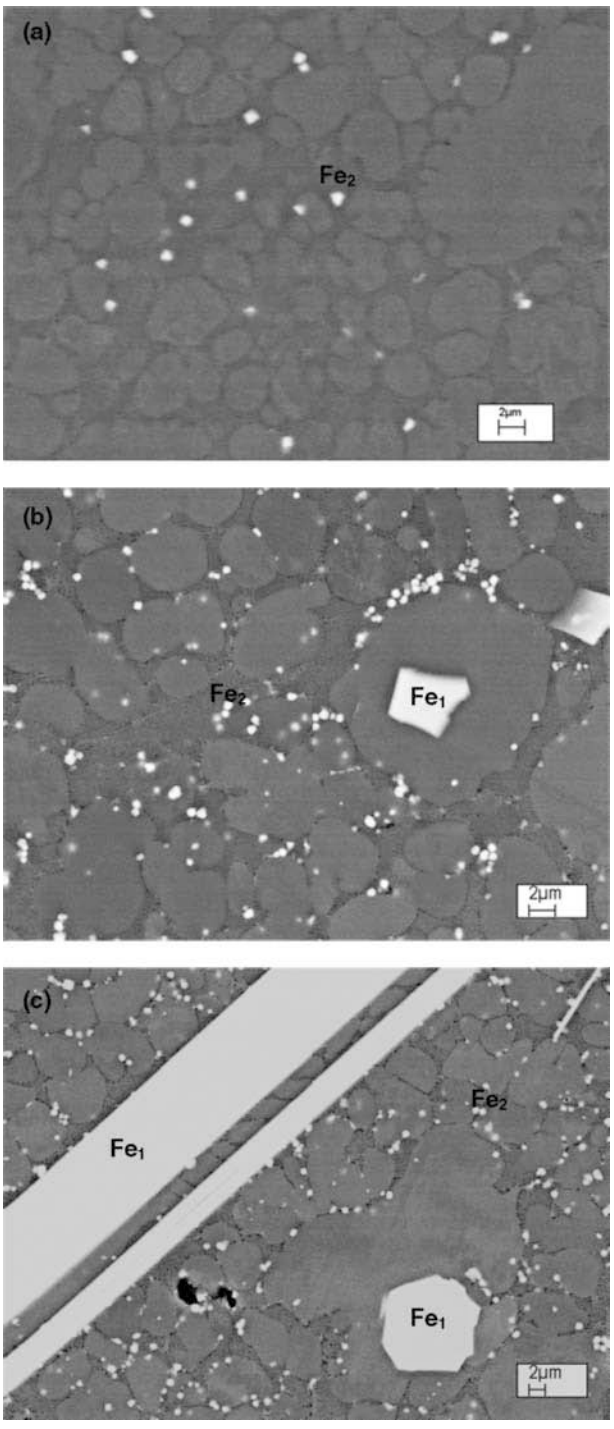

Figure 2. Backscattered SEM micrographs showing the morphology of Fe-rich intermetallics in the Al-5wt.%Mg-2wt%Si-0.54wt.%Mn diecast alloy with different amounts of Fe, (a) 0.21wt.%Fe, (b) 0.61 wt.% Fe, (g) 1.86 wt.% Fe

When the Fe contents in the alloys were increased to a level of 0.61wt.%Fe, there were two types of Fe-rich intermetallics observed. The Fe-rich intermetallics were formed in the shot sleeve and the die cavity, which were labelled as 'Fe_1' and 'Fe_2' respectively. The Fe_1-rich intermetallics were usually associated with the primary α-Al phase solidified in the shot sleeve and exhibited coarse compact morphology, which were found in tetragonal, pentagonal, hexagonal shapes. EDX quantification has identified the Fe-rich intermetallics to be the α-AlFeMnSi phase with the typical composition of α-$Al_{12}(Fe,Mn)_3Si$. Meanwhile, the fine intermetallics (labelled as Fe_2) were associated with α-Al phase solidified in the die cavity and segregated in the primary α-Al grain boundaries, which were identified by EDX quantification to be the same α-AlFeMnSi phase with the typical composition of α-$Al_{12}(Fe,Mn)_3Si$.

When the Fe contents in the alloys was further increased to a level of 1.86wt.% in Al-Mg-Si-Mn-Fe system, as shown in Fig.2c. A large fraction of needle-shaped Fe-rich intermetallics were found in the microstructure, in addition to the compact Fe-rich phase. The coarse and the fine compact primary Fe-rich intermetallics were identified by EDX quantification as the α-AlFeMnSi phase with the typical formula of α-$Al_{12}(Fe,Mn)_3Si$. The long needle-shaped Fe-rich compounds were quantitively confirmed as β-AlFe phase with the typical composition of β-$Al_{13}(Fe,Mn)_4Si_{0.25}$.

In the as-cast microstructure, some coarse Fe-rich intermetallics developed into more complex morphologies such as star-like shapes in associated with primary α-Al phase, as shown in Fig. 3. These Fe-rich intermetallics have been found in the castings with experimental composition of Fe>0.61wt. % and identified as α-AlFeMnSi phase with the typical composition of α-$Al_{12}(Fe,Mn)_3Si$. It was also found that the star-like α-AlFeMnSi phase were usually associated with α-Al phase formed in the shot sleeve. The results indicate that the solidification environments, especially the cooling rate in the shot sleeve is capable of producing different morphologies of primary α-AlFeMnSi phase. From these observations, the Fe-rich compounds of the compact and needle-shaped morphologies were identified as the α-AlFeMnSi and β-AlFe phase respectively. The intermetallic compounds in the Al-Mg-Si-Mn-Fe system are

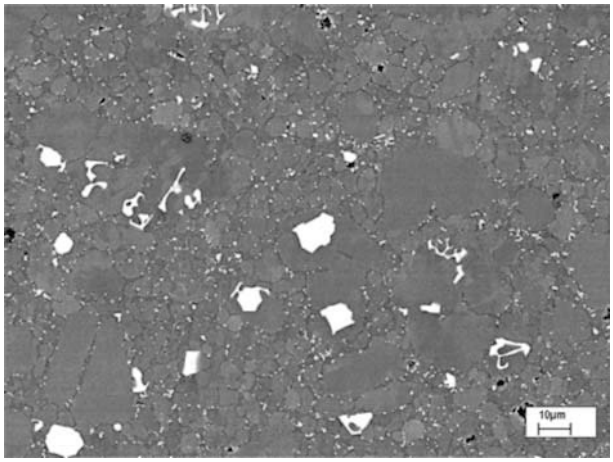

Figure 3. Backscattered SEM micrograph showing the morphology of Fe-rich intermetallics in the diecast Al-5Mg-2Si alloy with 0.54Mn and 0.84Fe

summarised in Table 2. It is seen that the primary α-$Al_{12}(Fe,Mn)_3Si$ intermetallics formed in the die cavity were observed in all diecast alloys in the experimental range. However, the primary Fe-rich intermetallics formed in the shot sleeve were significantly affected by the Fe contents. It is noticeable that the intermetallic β-$Al_{13}(Fe,Mn)_4Si_{0.25}$ phase formed in the experimental alloys were different to the intermetallic β-Al_5FeSi and β-AlFeSi phases observed in Al-Si, Al-Si-Cu and Al-Si-Mg alloys [8,9,12]. However, the cubic α-AlFeMnSi phase of α-$Al_{12}(Fe,Mn)_3Si$ intermetallics formed in the experimental alloys was found to be very similar to α-$Al_{15}(FeMn)_3Si_2$ intermetallics formed in Al-Si, Al-Si-Cu and Al-Si-Mg alloys [8,9,12].

The measured α-AlFeMnSi particles were consistently at 0.76 μm in diameter and no significant variation within the experimental ranges. However, the volume fraction of the fine Fe-rich particles increased with the increase of Fe contents in the alloys. As the fine Fe-rich particles were formed during the solidification in the die cavity under high cooling rate, the sizes of the Fe-rich intermetallics were mainly determined by the increased undercooling, enhanced heterogeneous nucleation and the shortened solidification time for the particle to grow.

Table 2. Average compositions of Fe-rich intermetallic phases measured by quantitive SEM/EDX analysis

Phase morphology	coarse compact	fine compact	large needle
Identified compounds	$Al_{12}(Fe,Mn)_3Si$	$Al_{12}(Fe,Mn)_3Si$ †	$Al_{13}(Fe,Mn)_4Si_{0.25}$
Al	76.64	75.47	75.62
Fe	11.83	12.16	19.20
Mn	5.95	6.28	3.81
Si	6.27	6.09	1.37
Fe/Mn	1.99	1.94	5.04

† The composition was further confirmed by TEM/EDX analysis

Mechanical Properties

Mechanical properties of the diecast Al-Mg-Si-Mn alloys with different Fe contents are presented in Fig. 4. It is seen that a slight enhancement in the yield strength and a significant detrimental to the elongation with the increase of Fe contents in the alloys. However, no obvious variation in the ultimate tensile strength was observed until Fe was higher than 0.6wt.% where it decreased. It is worth for a further emphasis that the enhancement of the yield strength for the diecast samples is less effective than the detrimental to the elongation of the same alloy in the experimental ranges. The overall increase of the yield strength of the diecast sample was 8% while the ultimate tensile strength decreased by 9% and the elongation decreased by 295%.

Discussion

CALPHAD of the multi-component Al-Mg-Si-Mn-Fe system

In order to understand the effect of alloying on solidification and microstructural evolution, CALPHAD modelling of the multi-component Al-Mg-Si-Mn-Fe system was carried out using PandaT software [20]. The Ti and other low levels of elements were not considered. The COST507 thermodynamic database [21] was used for constituent alloy systems and the α-AlFeMnSi was treated as a stoichiometric phase during the modelling. The calculated equilibrium phase diagrams on the cross sections of Al-5Mg-2Si-0.5Mn-xFe and are shown in Fig. 5. The calculated diagram can be divided into several regions with different Fe contents. The phase formation follows:

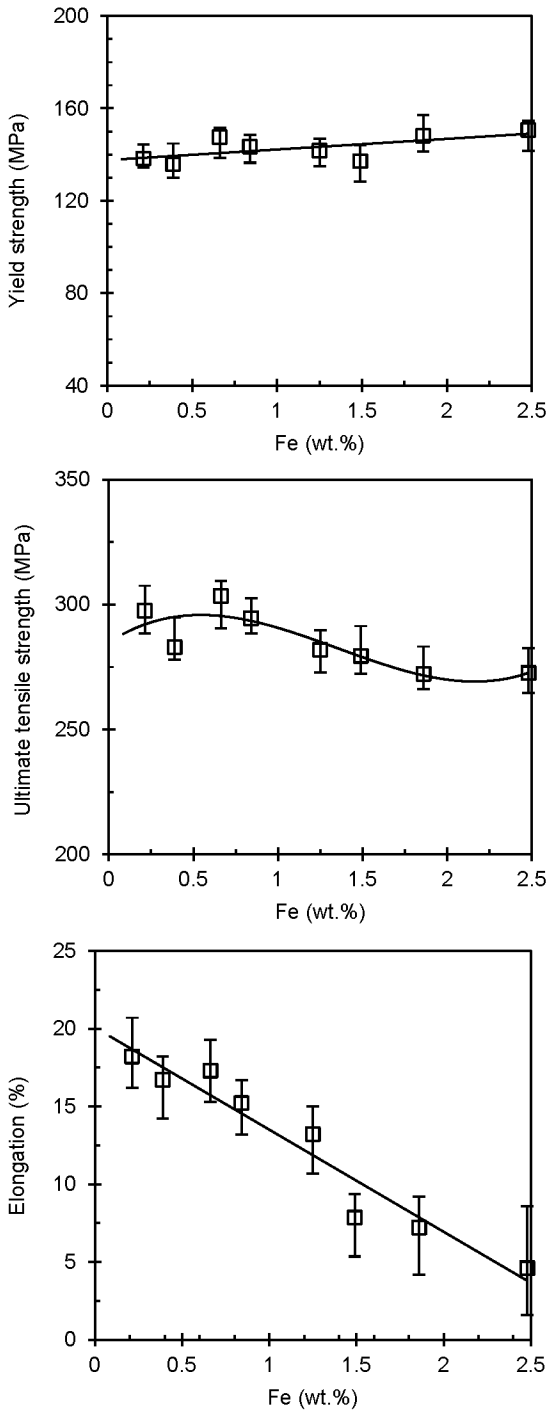

Figure 4. Effect of Fe content on the mechanical properties of die cast Al-Mg-Si alloys with different amounts of Mn, (a) yield strength, (b) ultimate tensile strength, and (c) elongation.

(1) L→ α-Al+α-AlFeMnSi+Mg_2Si with prior α-Al phase at Fe<(0.25wt.%), and
(2) L→ α-AlFeMnSi+α-Al+Mg_2Si with prior α-AlFeMnSi phase at 0.21wt.%<Fe<1.4wt.%, and
(3) L→β-AlFe +α-AlFeMnSi+α-Al+Mg_2Si with prior β-AlFe phase at Fe>1.4wt.%.

Phase formation in diecast Al-Mg-Si-Mn alloy

The solidification process and the associated changes of liquid compositions determine the formation of different phases. From the phase diagram in Fig. 5, it is seen that the prior phase is α-Al phase when Fe content is less than 0.25wt.%. The solidification starts to precipitate the α-Al phase in the shot sleeve, which is interrupted during die filling. The precipitation of α-Al phase continues in the die cavity, during which Si, Fe and Mn elements are enriched in the remaining liquid and the Fe-rich intermetallics are consequently formed in the melt. The high cooling rate in the die cavity and the absence of superheat in the melt enhance the heterogeneous nucleation, and therefore promote the formation of fine compact α-AlFeMnSi intermetallics. When Fe content is increased to a higher level, the prior phase becomes α-AlFeMnSi. The precipitation of α-AlFeMnSi compounds increases the undercooling in front of the interface of the crystal, resulting in the nucleation and growth of α-Al phase in associated with α-AlFeMnSi compounds. The solidification continues in the die cavity, where the compact α-AlFeMnSi compounds and α-Al phase precipitate under high cooling rate. When Fe content is further increased, the prior phase is β-AlFe phase. The precipitation of β-AlFe compounds consumes Fe element in the melt and thus alters the local melt composition with enriched Si and Mn, resulting in an increase of Mn/Fe ratio. When Mn/Fe ratio reaches the limitation, α-AlFeMnSi compound precipitates from the melt. The following solidification precipitate the α-AlFeMnSi and β-AlFe compounds. Overall, the formation of α-AlFeMnSi and β-AlFe phases consumes Fe, Mn, Si prior to the eutectic solidification. The final stage of solidification of the alloys is the multi-eutectic transformation to generate the eutectic structure mainly of Al-Mg_2Si eutectic phase.

Mn is largely consumed by the formation of the Fe-rich intermetallics. Therefore, an adequate level of Mn is necessary in order to maintain high Mn/Fe ratio for the formation of the cubic α-AlFeMnSi phase. In the observed α-AlFeMnSi intermetallics, the typical composition is α-$Al_{12}(Fe,Mn)_3Si$, which is made of less Si than that in the common α-$Al_{15}(FeMn)_3Si_2$ compounds. The main reason can be attributed to the low Si concentration in the alloy and the short of Si supply during solidification. In the experimental results, it is also confirmed that Mn/Fe=0.5 is necessary to suppress the formation of the β-AlFe compounds in the as-cast microstructure. β-AlFe intermetallics is immediately observed in the alloys when Mn/Fe<0.5, which is in good agreement with the observation in other alloys including Al-Si, Al-Si-Cu and Al-Si-Mg alloys [10-17]. However, α-AlFeMnSi phase can still be observed at low Mn/Fe ratio. Therefore, the Mn/Fe ratio can be used as an indicator for the formation of β-AlFe compounds, but not for determining the formation of α-AlFeMnSi phase.

Microstructure-property relationship

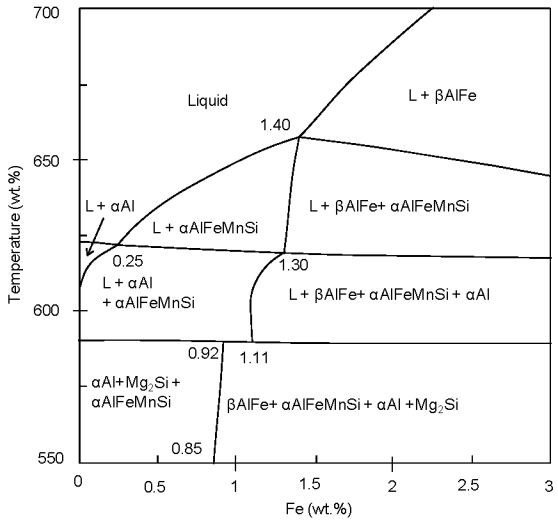

Figure 5. Cross section of equilibrium phase diagram of Al-5Mg-2Si-0.6Mn-xFe calculated by Pandat software.

In the results, the higher the iron concentrations in the alloy, the significantly more the elongation decreases. This is accompanied by a slight enhancement of the yield strength at increased iron level in the alloys. The ultimate tensile strength maintains at similar level when Fe is less than 0.6wt. %, but it decreases significantly when the Fe contents further increases. Meanwhile, a slight enhancement of the yield strength is also observed in the alloy with Mn addition compare to that in the alloy without Mn addition.

Referring to the solidification microstructure, the enhanced yield strength is believed to correspond to the increased amounts of Fe-rich intermetallic compounds, especially the fine intermetallics present at the α-Al grain boundaries. The increase in yield strength is accompanied with decreasing elongation as the added reinforcement due to the Fe-rich compounds is at the cost of the alloy ductility. Therefore the detrimental effect of iron content on the mechanical properties in the diecast Al-Mg-Si alloys should be determined mainly by the loss in ductility.

Conclusions

In high pressure die casting of Al-Mg-Si-Mn alloys, the formation of Fe-rich intermetallics occurs into two solidification stages. One is in the shot sleeve at lower cooling rates, and the other is in the die cavity at higher cooling rates. The Fe-rich intermetallics formed in the shot sleeve exhibit coarse compact, star-like or needle/plate shape morphology with varied sizes. The Fe-rich intermetallics formed in the die cavity are characterised by fine compact morphology with the size less than 3 μm.

In diecast Al-Mg-Si-Mn alloys, the prior phase is α-Al when Fe is less than 0.25wt.%, but the prior phase is β-$Al_{13}(Fe,Mn)_4Si_{0.25}$ when Fe is higher than 1.24wt.%. Over the Fe contents range from 0.25 to 1.24wt%, α-$Al_{24}(Fe,Mn)_6Si_2$ precipitates as prior phase to form either coarse compact compounds in the shot sleeve or fine compact particles in the die cavity.

The morphology and size of α-$Al_{12}(Fe,Mn)_3Si$ intermetallics are dependent on the cooling rate. The higher cooling rate in the die cavity enables the α-$Al_{12}(Fe,Mn)_3Si$ phase to solidify in a fine compact morphology. However, the lower cooling rate in the shot sleeve results in the formation of compact and star-like Chinese script α-$Al_{12}(Fe,Mn)_3Si$ phase in the as-cast microstructure.

Fe-rich intermetallics significantly affect the mechanical properties of the alloy castings. The higher the iron concentrations in the alloy, the more significantly the ductility reduces. This is accompanied by a slight enhancement of the yield strength. The ultimate tensile strength maintains the similar level when Fe contents is less than 0.6wt.%, but decreases significantly with the further increase of Fe contents in the diecast alloys.

Acknowledgement

The authors acknowledge the EPSRC and JLR for financial support.

References

[1] L. Wang, M. Makhlouf, D. Apelian, Int. Mater. Rev. 40(1995) 221-238.
[2] J. L. Jorstad, Die Casting Engineer (Nov/Dec 1986) 30-36.
[3] Z. Yi, Y.X. Gao, P.D. Lee, T.C. Lindley, Mater. Sci. Eng. A386 (2004) 396-407.
[4] G.B. Winkelman, Z.W. Chen, D.H. StJohn, M.Z. Jahedi, J. Mater. Sci. 39(2004)519-528.
[5] X. Fang, G. Shao, Y.Q. Liu, Z. Fan, Mater. Sci. Eng. A 445-446 (2007) 65-72.
[6] S. S. Kumari, R. M. Pillai, B. C. Pai, K. Nogita, A. K. Dahle, Metall. Mater. Trans. A 37A (2006) 2581-2587.
[7] L. A. Narayanan, F. H. Samuel, J. E. Gruzleski, Metall. Mater. Trans. A 26A (1995) 2161-2174.
[8] P. Skjerpe, Metall. Mater. Trans. A 18A (1987) 189-200.
[9] L. F. Mondolfo, Aluminium Alloys: Structure and Properties, (Butterworth, London, 1976) pp.534.
[10] L. Backerud, G. Chai, J. Tamminen, Solidification Characteristics of Aluminium Alloys, Foundry Alloys Vol. 2 (AFS/Skanaluminum, 1990) pp. 71- 84.
[11] S. Shivkumar, L. Wang, D. Apelian, JOM 43 (1991) 26 -32.
[12] M.V. Kral, H.R. McIntyre, M.J. Smillie, Scripta Mater. 51 (2004) 215-219.
[13] J.G. Zheng, R. Vincent, J.W. Steeds, Philos. Mag. 79 (1999) 2725 -2733.
[14] K.Y. Wen, W. Hu, G. Gottstein, Mater. Sci. Technol. 19 (2003) 762 -768.
[15] A. Couture, AFS Int. Cast Met. J. 6 (1981) 9-17.
[16] G. K. Sigworth, S. Shivkumar and D. Apelian, AFS Trans. 97 (1989) 811-824.
[17] A. Pennors, A. M. Samuel, F. H. Samuel, H. W. Doty, AFS Trans. 106 (1998) 251-264.
[18] S. Murali, K. S. Raman and K. S. S. Murthy, Cast Metals 6 (1994) 189-198.
[19] A. M. Samuel, A. Pennors, C. Villeneuve, F. H. Samuel, Int. J. Cast Metals Res. 13 (2000) 231-253.
[20] S.-L. Chen, S. Daniel F. Zhang, Y. A. Chang, X.-Y. Yan, F.-Y. Xie, R. Schmid-Fetzef, W. A. Oatesd, Calphad 26(2002)175-188.
[21] I. Ansara, A.T. Dinsdale, M. H. Rand (eds.), COST 507-final report: Thermodynamic Database for Light Metal Al-alloys, vol.2, European Communities, Brussels 1998.